Direct Control of Brown Adipose Tissue Thermogenesis by Central Nervous System Glucagon-Like Peptide-1 Receptor Signaling

Sarah H. Lockie,[1,2] Kristy M. Heppner,[1] Nilika Chaudhary,[1] Joseph R Chabenne,[3] Donald A. Morgan,[4] Christelle Veyrat-Durebex,[5] Gayathri Ananthakrishnan,[1] Françoise Rohner-Jeanrenaud,[5] Daniel J. Drucker,[6] Richard DiMarchi,[3] Kamal Rahmouni,[4] Brian J. Oldfield,[2] Matthias H. Tschöp,[1] and Diego Perez-Tilve[1]

We studied interscapular brown adipose tissue (iBAT) activity in wild-type (WT) and glucagon-like peptide 1 receptor (GLP-1R)–deficient mice after the administration of the proglucagon-derived peptides (PGDPs) glucagon-like peptide (GLP-1), glucagon (GCG), and oxyntomodulin (OXM) directly into the brain. Intracerebroventricular injection of PGDPs reduces body weight and increases iBAT thermogenesis. This was independent of changes in feeding and insulin responsiveness but correlated with increased activity of sympathetic fibers innervating brown adipose tissue (BAT). Despite being a GCG receptor agonist, OXM requires GLP-1R activation to induce iBAT thermogenesis. The increase in thermogenesis in WT mice correlates with increased expression of genes upregulated by adrenergic signaling and required for iBAT thermogenesis, including *PGC1a* and *UCP-1*. In spite of the increase in iBAT thermogenesis induced by GLP-1R activation in WT mice, $Glp1r^{-/-}$ mice exhibit a normal response to cold exposure, demonstrating that endogenous GLP-1R signaling is not essential for appropriate thermogenic response after cold exposure. Our data suggest that the increase in BAT thermogenesis may be an additional mechanism whereby pharmacological GLP-1R activation controls energy balance.

The increasing incidence of type 2 diabetes (T2D) and obesity worldwide has prompted the need for new therapies. Agonism of the receptor for glucagon-like peptide-1 (GLP-1) is currently one of the most successfully and widely used therapies for T2D. GLP-1 is a product of proglucagon that also gives rise to glucagon (GCG) and oxyntomodulin (OXM) (1). Both GLP-1 and its receptor (GLP-1R) are expressed in peripheral tissues and in areas of the central nervous system (CNS) involved in the control of energy balance. Treatment with GLP-1R agonists improves glycemic control and reduces body weight in diabetic humans (2). Studies in animals have demonstrated that CNS–GLP-1R signaling contributes to the body weight–reducing effect of these agonists (3).

GCG is produced in the α cells of the pancreatic islets and is involved in the maintenance of euglycemia. Although its exogenous administration induces body weight loss associated with anorexia and increased energy expenditure (4), GCG has been traditionally dismissed as a potential drug target because of its diabetogenic effects. However, recent preclinical data have shown that simultaneous activation of both GLP-1R and GCG receptor (GCGR) leads to greater efficacy in both glycemic control and weight loss than the activation of GLP-1R alone (5,6).

OXM can bind to and activate both GLP-1R and GCGR (7), and studies with rodents (8,9) and humans (10) suggest that it may be efficacious in treating obesity and diabetes. OXM regulates feeding, at least in part, through GLP-1R (7,11). There is evidence that OXM action in the CNS reduces body weight by increasing energy expenditure (12). This may involve activation of brown adipose tissue (BAT) metabolism, since intracerebroventricular (ICV) administration of OXM reduces the weight of interscapular BAT (iBAT) pads and increases body temperature in rats (12). The relative contribution of GLP-1R and GCGR to this process has never been investigated; however, it is known that GCG regulates iBAT activity, and this may be, at least in part, centrally mediated (13). The contribution of GLP-1R to the control of energy expenditure, and more specifically to BAT metabolism, remains largely unknown.

The sympathetic nervous system (SNS) is essential for control of BAT metabolism by the CNS (14) and is involved in the CNS–GLP-1R control of lipid metabolism in white adipose tissue (WAT) (15). This, in addition to the evidence that GCG may increase BAT thermogenesis through actions in the CNS (13), led us to hypothesize that the action(s) of GCGR and GLP-1R in the brain controls BAT thermogenesis through the SNS. Here, we show that central administration of both GCGR and GLP-1R agonists increased SNS activity to iBAT and induced thermogenesis. Thus, we propose that CNS–GLP-1R may contribute to the control of energy balance by regulating BAT thermogenesis. The existence of functional BAT in adult humans has now been determined (16–18), and effort needs to be directed toward a better understanding of the regulation of this tissue as a target for antiobesity therapeutics. The increase in BAT metabolism described here

may contribute to the weight loss induced by GCGR and GLP-1R agonists in both animal models and humans.

RESEARCH DESIGN AND METHODS

Peptide synthesis. Peptides were synthesized as previously described (6). We used native GLP-1-(7-36)NH$_2$ and OXM. In order to increase the solubility of GCG, we substituted aspartic acid for an asparagine at position 28 and a glutamic acid for a threonine at position 29. The resulting GCG (Asn28, Thr29) was tested in vitro using human embryonic kidney 293 cells cotransfected with the GCGR as previously described (6), and its ability to stimulate cAMP production was indistinguishable from native GCG.

Animals. We used single-housed male 12- to 14-week-old C57BL/6J mice (The Jackson Laboratory) or GLP-1R knockout (*Glp1r$^{-/-}$*) mice, generated as previously described (19) and bred at the University of Cincinnati. Mice were maintained on a 12:12-h light-dark cycle at 22°C with free access to water and to either a standard chow (Harlan Teklad) or a diabetogenic diet (58% kcal from fat; Research Diets) as indicated. All studies were approved by and performed following the guidelines of the institutional animal care and use committees of the University of Cincinnati, University of Iowa, University of Geneva, and Monash University.

Administration of peptides and fasting

Chronic ICV infusion. ICV minipumps (Alzet; Durect, Cupertino, CA) were implanted as previously described (20). The vehicle for GLP-1 and OXM was saline, whereas the vehicle for GCG was PBS. Doses are as specified in RESULTS.

Acute ICV injection. ICV cannulae were placed as previously described (20) and secured with glue (Tarzan's grip) and dental cement. Mice were lightly restrained using a cloth, and the peptides were administered through an injector inserted into the guide cannula at a dose of 1 nmol (GLP-1 and OXM) or 0.4 nmol (GCG) in 1.5 uL vehicle. Previous reports demonstrate that comparable ICV doses of GLP-1 (21) and OXM (9) reduce feeding in rats.

The injector was left in place for 20 s before removal. Injections were performed just before the onset of the dark phase.

Intraperitoneal injection. Mice were injected intraperitoneally before the dark phase with equimolar amounts of peptides as administered in the acute ICV studies—just in a volume of 200 uL vehicle.

Fasting/refeeding. Just before the onset of the dark phase, food was removed from the fasting group. At the onset of light, they received back 2 g of food, which was the average amount consumed in 24 h by the GLP-1– and OXM ICV–treated mice in previous experiments.

BAT sympathetic nerve recordings. We measured sympathetic nerve activity (SNA) in iBAT in mice 1 week after implantation of an ICV cannula. A nerve fascicle projecting to the iBAT pad was isolated, and the recording and anesthesia protocols were carried out as previously described (15). Baseline SNA was recorded for 10 min followed by ICV administration of vehicle (2 μL) or peptide. (GLP-1 and OXM were administered at 1 and 0.1 nmol in 2 μL saline, and GCG was administered at 0.4 nmol in 2 μL PBS.) SNA responses to GLP-1, OXM, GCG, and vehicle were recorded continuously for 240 min; after this procedure, mice were killed with a lethal dose of ketamine/xylazine. The integrated voltage after death (background noise) was subtracted from the total integrated voltage to calculate actual iBAT SNA.

BAT temperature telemetry. Temperature-sensitive transmitters (E-mitters; Mini Mitter, Bend, OR) were implanted into a blunt-dissected pocket underneath the iBAT through a 1-cm incision made posterior to the scapulae either simultaneously (for chronic infusion) or 3 days after implantation of ICV cannula (for acute injections). Data were collected via receiver plate (ER-4000; Minimitter). For determination of alterations in iBAT temperature in response to the decreasing environmental temperature, probes were implanted as above; however, mice were housed in chambers with integrated control of ambient temperature and simultaneous measurement of food intake, locomotor activity, and energy expenditure by indirect calorimetry (TSE Systems, Chesterfield, MO).

Euglycemic-hyperinsulinemic clamps. Mice were fitted with ICV cannula and minipumps administering 2.5 nmol/day GLP-1, OXM, or vehicle as described above. Food intake and body weight were monitored for 3 days. To control for the effect of weight loss on insulin responsiveness, we pair-fed a group of mice to the GLP-1 treatment group. Mice were then reanesthetized (80 mg/kg pentobarbital sodium salt, Esconarkon; Streuli Pharma, Uznach, Switzerland) without previous fasting, and euglycemic-hyperinsulinemic clamps were performed as previously described (22). Hepatic glucose production and glucose infusion rate to maintain euglycemia were measured under basal and insulin-stimulated conditions (18 mU/kg, Actrapid HM; Novo Nordisk Pharma, Zurich, Switzerland) using D-[3-^{3}H]glucose (16.6 μCi/kg/min; Perkin Elmer, Waltham, MA).

Quantitative PCR. RNA from iBAT, WAT, and liver was extracted using a commercially available kit (RNeasy; Qiagen, Valencia, CA) following the manufacturer's instructions. After DNase I treatment (Invitrogen, Carlsbad, CA), cDNA was synthesized using SuperScript-III (Invitrogen), and gene expression was determined by quantitative PCR using gene-specific TaqMan

assays (Life Technologies, Carlsbad, CA). Gene expression was evaluated using the Δ-Δ C$_t$ method. The housekeeping gene was *HPRT*.

Plasma measurements. Triiodothyronine (T3) levels were determined by RIA (MP Biomedicals, Cleveland, OH) following the manufacturer's instructions.

Statistical analysis. Data are presented as means ± SEM. Student *t* test for independent samples was used for comparisons between two groups. Two-way ANOVA followed by Bonferroni correction test or Tukey post hoc test was used for comparisons between multiple, independent groups.

RESULTS

ICV GLP-1, OXM, and GCG significantly reduced food intake and body weight over a 4-day period as expected (Fig. 1). Infusion of either GLP-1 or OXM at 0.75 nmol/day in chow-fed and diet-induced obese (DIO) mice significantly decreased food intake (Fig. 1*A* and *B*) and body weight
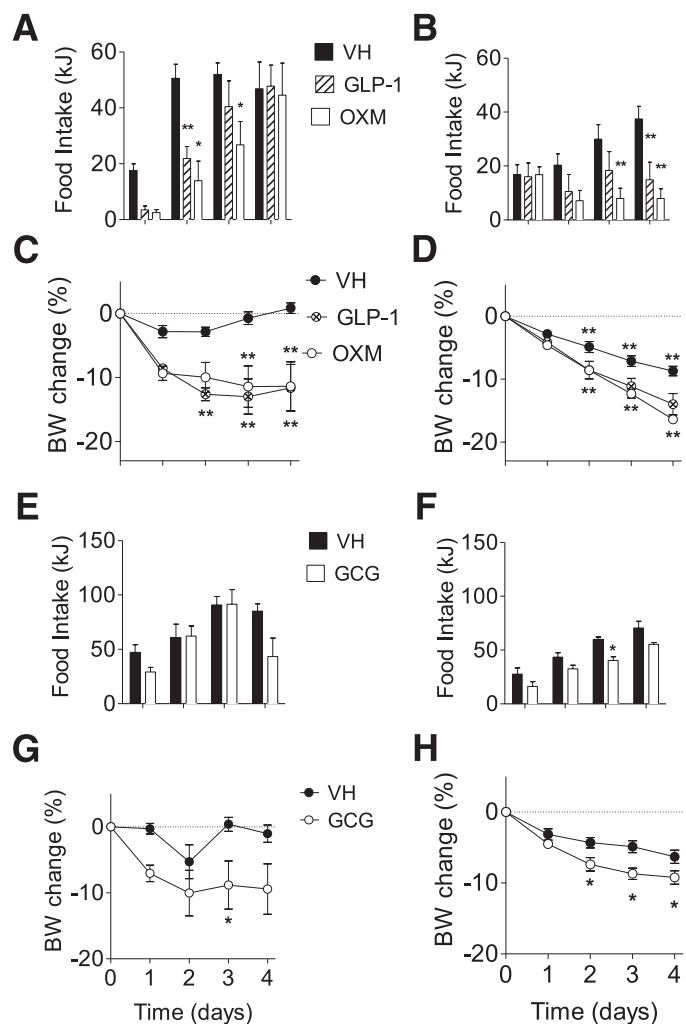

FIG. 1. Central chronic infusion of GLP-1R and GCGR agonists induces sustained body weight (BW) loss. ICV GLP-1 and OXM significantly reduced feeding (*A*, chow fed and *B*, DIO) and body weight (*C*, chow fed and *D*, DIO) in chow-fed and high-fat diet (HFD)-fed DIO mice. ICV GCG did not affect feeding in lean chow-fed mice (*E*) but reduced food intake in DIO mice (*F*). Despite the lack of an anorectic effect, ICV GCG significantly reduced body weight in lean chow-fed mice (*G*) and in DIO mice (*H*). Data are expressed as mean ± SE percentage of change (for body weight) or kilojoules (kJ) (for food intake) vs. the corresponding control group (*n* = 6–8). A significant main effect was required before post hoc testing. (*P* < 0.05, two-way repeated-measures ANOVA.) **P < 0.01, *P < 0.05 vs. corresponding vehicle (VH); two-way ANOVA with Bonferroni post hoc test. For *C* and *D*, the asterisks above relate to OXM, and those below relate to GLP-1.

(Fig. 1*C* and *D*) across the 4 days. GCG was infused at 0.4 nmol/day because of limitations of solubility. At this dose, GCG reduced feeding only in DIO mice (Fig. 1*E* and *F*). However, ICV GCG significantly reduced body weight in both chow- and high-fat–fed mice (Fig. 1*G* and *H*) ($P <$ 0.05). This decrease in body weight is consistent with increased energy expenditure previously attributed to GCG (4).

Given that one of the mechanisms by which GCG induces energy expenditure is by activating iBAT thermogenesis, we measured iBAT temperature after an acute ICV injection of GCG in mice. ICV GCG (bolus dose of 0.4 nmol) caused a trend toward increased iBAT thermogenesis across a 24-h recording window ($P = 0.08$) (Fig. 2*A*). Consistent with its activity as GCGR agonist, ICV administration of OXM significantly increased iBAT temperature during the 24 h after injection (Fig. 2*B*). Interestingly, ICV GLP-1 injection also increased iBAT temperature (Fig. 2*C*). The average iBAT temperature across the first half of the dark phase was significantly higher for all three peptides (Fig. 2*D–F*). Again, GCG did not affect feeding (Fig. 2*G*). The increase in iBAT temperature induced by ICV OXM or GLP-1 occurred despite the profound suppression of food intake assessed 2 h post injection (Fig. 2*H* and *I*). Food intake at 24 h was not different from vehicle-treated controls for any group (data not shown).

Our expectation was that reduced food intake associated with fasting would normally cause a decrease in thermogenesis as an energy-preservation mechanism; however, to rule out the possibility that the reduced food intake itself could drive an increase in iBAT temperature, we performed an experiment designed to mirror the feeding behavior of the GLP-1– and OXM-treated mice. Fasting during the dark phase significantly lowered iBAT temperature by the end of the 12-h period ($P < 0.05$), and the reinstatement of food completely restored normal iBAT temperature (Fig. 2*J*). In contrast to ICV injection, intraperitoneal administration of equimolar doses of the peptides did not increase iBAT temperature (Fig. 2*K*), further suggesting that this effect requires signaling at the CNS.

Home cage locomotion remained unchanged either after ICV GCG (Fig. 4*M*) or OXM (Fig. 4*L*) or after fasting (Fig. 4*O*) but was significantly suppressed during the first hour after ICV GLP-1, consistent with previous findings in rats (21).

SNA is a necessary component of CNS-mediated BAT thermogenesis. We measured SNA from the nerves innervating iBAT after acute ICV administration of the peptides. All peptides increased iBAT-SNA (Fig. 3*A–C*). The average SNA for the final hour of recording was significantly higher for all groups (Fig. 3*D–F*), demonstrating that GCG, OXM, and GLP-1 are capable of independently increasing sympathetic drive to iBAT.

Given that both GLP-1R and GCGR bind OXM and since we had demonstrated that the cognate ligands for both receptors increase iBAT thermogenesis, we used mice with genetic disruption of the *Glp1r* to identify the relative contribution of this receptor to OXM's thermogenic capacity. To this end, we infused OXM into GLP-1R knockout mice ($Glp1r^{-/-}$). In contrast to a robust thermogenic OXM response in the WT littermate controls (Fig. 4*A*), $Glp1r^{-/-}$ mice had no thermogenic response to OXM when they were continuously infused by mini-pump (Fig. 4*B*). The average iBAT temperature in OXM-treated WT mice was significantly higher than in vehicle-treated mice during both the dark and light phases (Fig. 4*C*), while there were no significant differences in the $Glp1r^{-/-}$ mice (Fig. 4*D*). The

sustained increase in iBAT temperature induced by ICV OXM did not correlate with plasma T3 levels (Fig. 4*E*). Importantly, the effect of ICV OXM on iBAT temperature persisted beyond the effect on food intake in the WT mice (Fig. 4*F*). As expected, there were no differences in feeding between groups in the $Glp1r^{-/-}$ mice (Fig. 4*G*). Likewise, ICV OXM did not alter locomotor activity (Fig. 4*H* and *I*).

To gain insights into the molecular mechanisms that mediate the thermogenic action of OXM, we assessed the effect of ICV OXM for 72 h on the iBAT gene expression profile in WT and $Glp1r^{-/-}$ mice. Given that during this period ICV OXM significantly reduced food intake and body weight (Fig. 1*A*), we pair-fed the WT vehicle control group to allow for comparisons independent of feeding effects. As a result of pair-feeding, both WT vehicle and OXM-infused mice lost a similar amount of weight during the duration of the infusion (WT saline −10.6 ± 0.4% vs. WT OXM −10.1 ± 1.8%; $Glp1r^{-/-}$ saline −3.4 ± 1% vs. $Glp1r^{-/-}$ OXM −4.3 ± 0.8%) (WT vs. knockout, $P < 0.001$). ICV OXM in WT, but not in $Glp1r^{-/-}$ mice, increased the expression of genes associated with higher thermogenic activity of BAT. Specifically, ICV OXM increased the expression of peroxisome proliferator–activated receptor γ coactivator 1-α (PGC1a) and its genetic target uncoupling protein 1 (UCP-1), the key protein responsible for thermogenesis in the mitochondria (Fig. 5*A* and *B*), although this increase did not result in a detectable change in UCP-1 protein content (data not shown). UCP-1 expression in the inguinal and retroperitoneal white fat pads was not altered (data not shown). ICV OXM also increased the expression of type II iodothyronine deiodinase (DIO2) in BAT, required for the intracellular conversion of thyroxine (T4) to 3,3′,5-triiodothyronine (T3) (Fig. 5*C*). Consistent with a higher adrenergic stimulation, ICV OXM significantly increased the expression of the metabolic regulator fibroblast growth factor 21 (FGF21) in iBAT (Fig. 5*D*). In contrast, *FGF21* gene expression levels did not increase in the inguinal or retroperitoneal fat pads or in the liver (data not shown). ICV OXM increased monocarboxylate transporter 1 (MCT1), GLUT4, and lipoprotein lipase (LPL), which are involved in the transport of metabolites across cell membranes (Fig. 5*E–G*). ICV OXM increased acetoacetyl-CoA synthetase (AACS) and fatty acid synthase (FASN) expression, suggesting that it stimulates lipogenesis in BAT. In contrast, ICV OXM did not affect the expression of carnitine palmitoyltransferase-1b (Fig. 5*J*), required for the transport of fatty acids inside of the mitochondria, or increased expression of genes involved in the iBAT differentiation (PRDM16) (Fig. 5*K*) or mitochondrial biogenesis (nuclear respiratory factor-1 [NRF-1]) (Fig. 5*L*).

In order to assess whether the increase in iBAT metabolism could be associated with changes in insulin responsiveness, we performed hyperinsulinemic-euglycemic clamps in mice treated ICV for 3 days with either GLP-1 or OXM or pair-fed to the GLP-1 group. ICV OXM and GLP-1 reduced body weight but did not significantly affect peripheral insulin responsiveness compared with pair-fed mice (Table 1). These data suggest that CNS–GLP-1R specifically regulates iBAT thermogenesis, independent of changes in food intake or glucose homeostasis.

In view of the significant and sustained increase in iBAT temperature induced by CNS–GLP-1R signaling, we hypothesized that GLP-1R may be required for the appropriate stimulation of iBAT metabolism by cold exposure. To test this, we compared the response of $Glp1r^{-/-}$ mice to their WT littermates when exposed to ambient cold. We
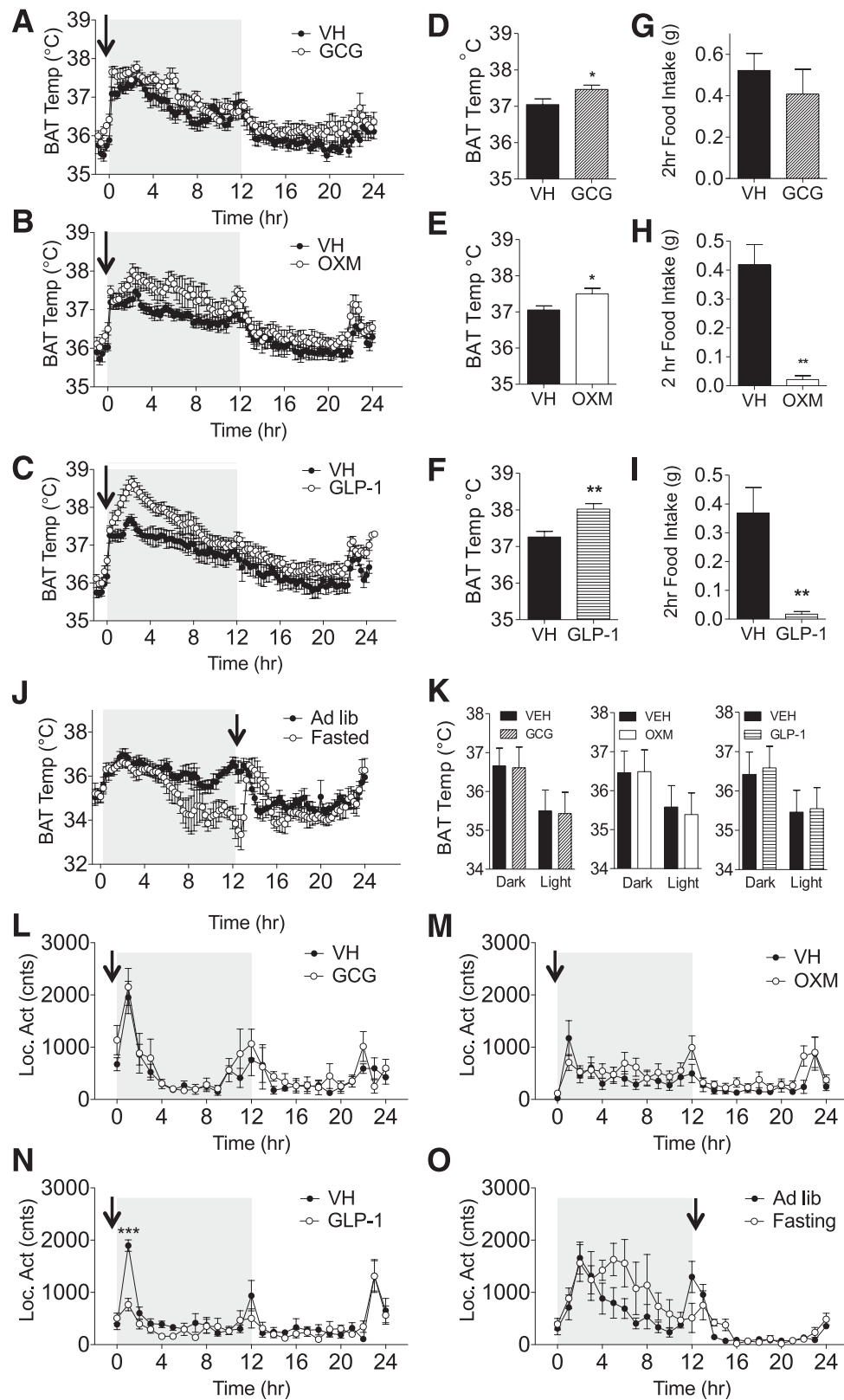
FIG. 2. Acute central injection of GLP-1R and GCGR agonists increases BAT thermogenesis. BAT temperature (Temp) was increased with acute ICV administration of GCG (*A*), OXM (*B*), and GLP-1 (*C*). Repeated-measures ANOVA showed significant main effects for GLP-1 and OXM and a main-effect *P* value of 0.08 for GCG across the 24-h period. Average iBAT temperature over the first half of the dark phase was significantly higher for all compounds (*ID-F*) as determined by a *t* test (*$P < 0.05$, **$P < 0.01$). Two-hour food intake after injection and onset of the dark phase was significantly depressed in OXM (*H*) and GLP-1 (*I*) but unaffected with GCG (*G*) as determined by a *t* test (**$P < 0.01$). *J*: 12 h of fasting significantly reduces iBAT temperature, with normal temperature reinstated after a meal (2 g chow, indicated by arrow); repeated-measures ANOVA shows significant main effect during the dark phase only ($P < 0.05$). *K*: Intraperitoneal injection of the same nanomole dose of peptides as used in *A–I* did not affect iBAT thermogenesis; individual *t* tests for each dark and light phase, $P > 0.05$. In contrast with ICV GLP-1 (*N*), ICV GCG, OXM, or food restriction did not significantly affect the home cage locomotor activity (Loc. Act) despite their effect on iBAT temperature (*L, M,* and *O,* respectively). Data are expressed as means ± SE (*n* = 6–8). ***$P < 0.01$ vs. vehicle (VH); two-way ANOVA with Bonferroni post hoc test. hr, hour; Ad Lib, ad libitum; cnts, counts.
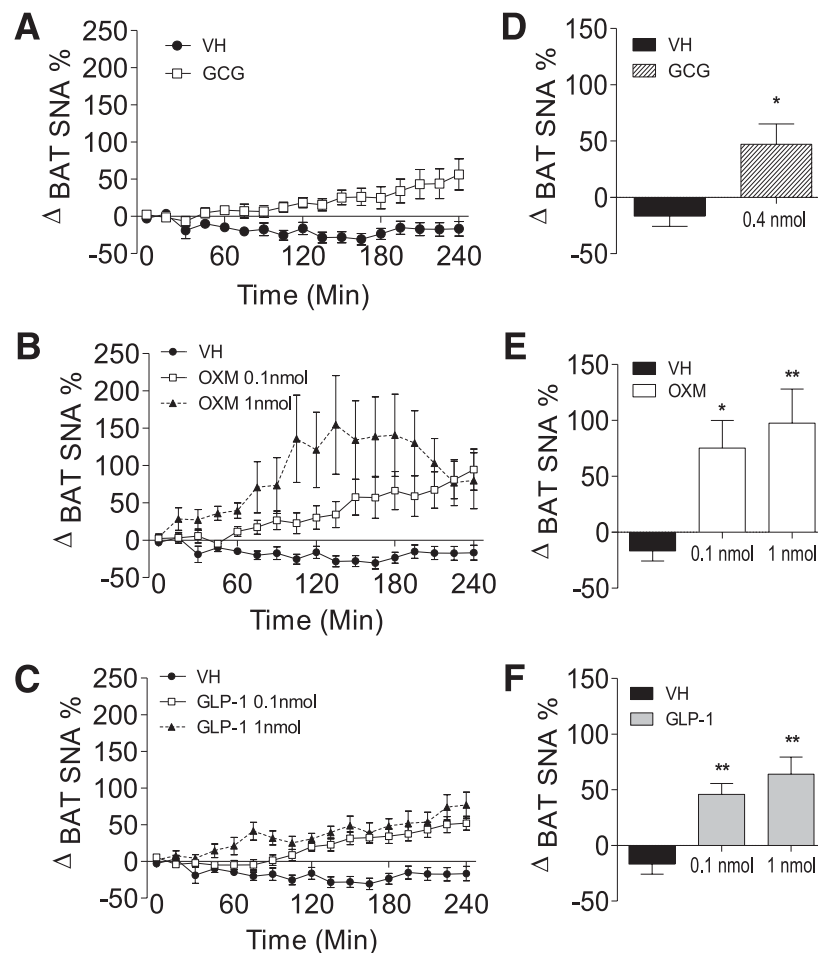
FIG. 3. Acute central injection of GLP-1R and GCGR agonists increases electrophysiological activity of the sympathetic fibers that innervate the iBAT. Activity of sympathetic nerves projecting to iBAT increased after acute ICV administration of GCG (*A*), OXM (*B*), or GLP-1 (*C*). Repeated-measures ANOVA shows a significant main effect for all compounds at all doses; $P < 0.01$. *D–F*: Histograms on the right show average % increase for final hour, which was significant for all compounds as determined by one-way ANOVA with Tukey post hoc (*D* and *E*) and Student *t* test (*F*) (*$P < 0.05$, **$P < 0.01$). Data are expressed as means ± SE ($n = 6–8$). VH, vehicle.

were not able to detect any differences in food intake, locomotor activity, whole-body energy expenditure, or iBAT temperature (Fig. 6*A–D*) between $Glp1r^{-/-}$ mice and WT littermates during extended, decremental cold exposure from 24 to 14°C. Additionally, both genotypes maintained a stable core temperature over 8 h of acute cold exposure at 4°C (Fig. 6*E*). However, since nonshivering thermogenesis is not essential for the maintenance of body core temperature (BCT) in response to an acute cold exposure (14), these data do not exclude the possibility that $Glp1r^{-/-}$ mice may have impaired activation of the thermogenic pathways in iBAT in response to an acute cold challenge. Therefore, we evaluated the expression of genes required for the activation of the iBAT thermogenesis in response to a 2-h cold exposure at 4°C in another cohort of lean, chow-fed WT and $Glp1r^{-/-}$ mice. Although the 2-h cold challenge was insufficient to induce higher *UCP-1* gene expression (Fig. 6*F*), it led to a significant increase in *PGC-1a* and *DIO2* expression in both WT and $Glp1r^{-/-}$ mice (Fig. 6*G* and *H*) compared with control mice maintained at room temperature. Despite similar body weights (WT 26.3 g ± 0.9 vs. knockout 24.4 g ± 0.9, $P > 0.05$) and adiposity (Fig. 6*I*), $Glp1r^{-/-}$ mice showed significantly higher iBAT mass (Fig. 6*J*). These data demonstrate that GLP-1R signaling is not essential for the activation of iBAT

in response to cold but suggest that it is required for normal control of iBAT function.

DISCUSSION

GLP-1R agonists are widely used for the treatment of T2D owing to their ability to improve glycemic control and to induce body weight loss. A new generation of drugs combining both GLP-1R and GCGR have demonstrated further potency in reducing body weight in preclinical animal models. Yet, the specific mechanisms whereby either the GLP-1R or GCGR contributes to the reduction of body weight are not completely understood. Here, we demonstrate that in addition to body weight loss, ICV administration of the preproglucagon-derived peptides GLP-1, OXM, and GCG increases iBAT thermogenesis by increasing SNS activity and without altering peripheral insulin responsiveness. Although GLP-1R activation potently induces iBAT thermogenesis, endogenous physiological GLP-1R signaling is not essential for normal induction of cold-induced iBAT thermogenesis. We propose that iBAT thermogenesis may be one of the multiple mechanisms by which, along with reduced food intake (21) and decreased lipid accumulation in WAT (15), pharmacological CNS–GLP-1R activation contributes to the maintenance of energy balance.
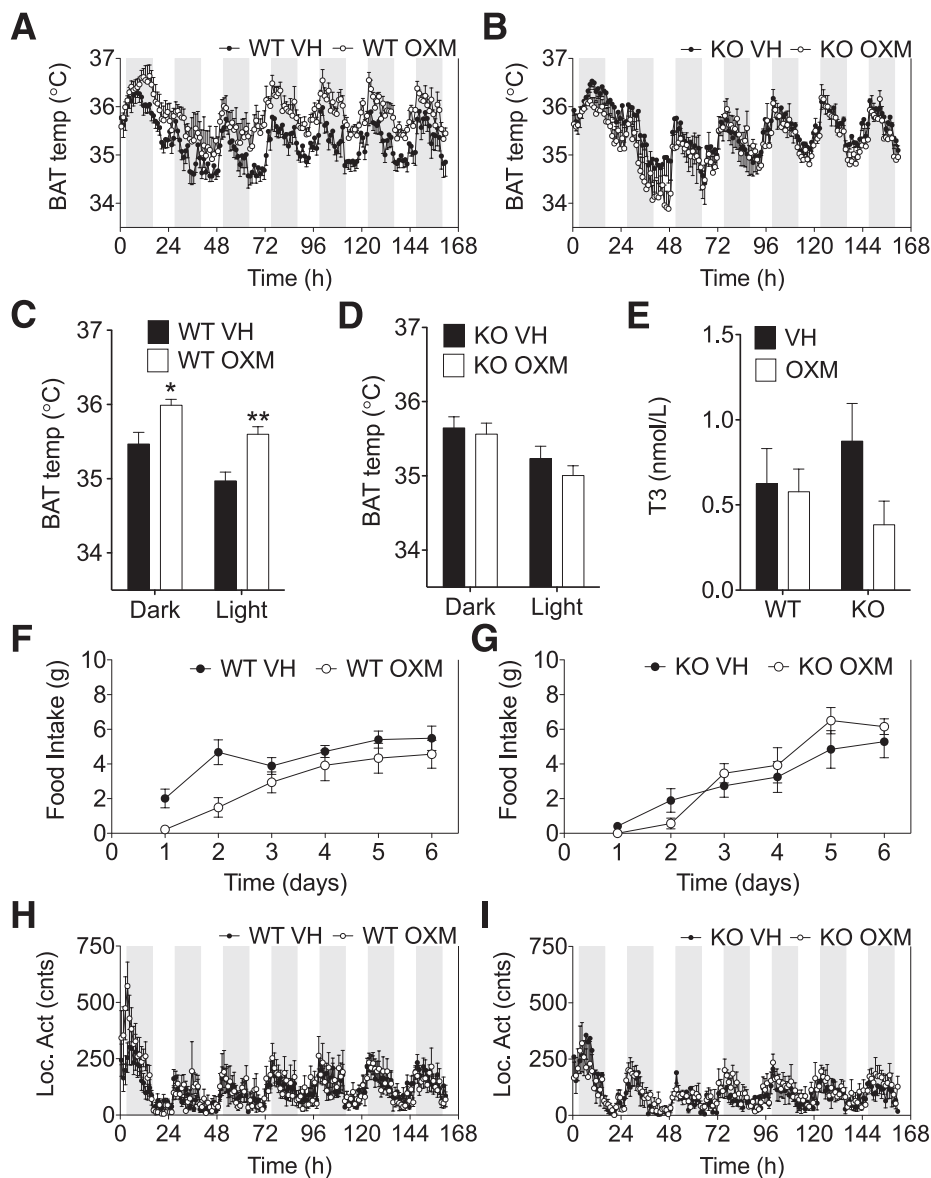
FIG. 4. Chronic CNS infusion of OXM induces a sustained increase in BAT thermogenesis that requires a functional GLP-1R. ICV infusion of OXM induces a sustained increase in iBAT thermogenesis over the course of 6 days in WT mice (*A*), which is completely absent in the *Glp1r*$^{-/-}$ mouse (*B*). The average increase over 5 days in iBAT temperature induced by OXM is significant in both the light and dark phases in WT mice (*C*) but not in the *Glp1r*$^{-/-}$ mice (*D*). The ICV OXM–induced iBAT thermogenesis does not correlate with increased plasma T3, as measured at the end of the study (*E*). Food intake (*F* and *G*) and home cage locomotor activity (Loc. Act) (*H* and *I*) of WT and *Glp1r*$^{-/-}$ mice during the period of ICV OXM infusion. Data are expressed as means ± SE (*n* = 6–8). *P < 0.05, **P < 0.01 vs. corresponding vehicle (VH); two-way ANOVA with Bonferroni post hoc test. KO, knockout; cnts, counts.

Although there is old evidence for the role of GCG in the control of energy balance, its low solubility has been a limiting factor for studying its effects in vivo. Here, we overcome that limitation by using a more hydrophilic GCG analog. The food intake–independent effect on body weight that we observed in ICV GCG–treated mice supports a role for GCG in stimulating energy expenditure. One of the proposed mechanisms by which GCG increases energy expenditure is through the activation of iBAT thermogenesis (23,24). Pretreatment with a β-adrenergic receptor antagonist abolishes the effect of GCG on oxygen consumption in rats in vivo, suggesting that the effect of GCG on iBAT may be attributed to, at least in part, the release catecholamines (25). Adrenergic signaling is a critical regulator of iBAT metabolism and is mainly provided to the iBAT by SNS innervation. Given that in our experiments acute ICV GCG increases both iBAT thermogenesis and the activity of the SNS fibers innervating the BAT, we suggest that the CNS mediates some of the effects of GCG on energy expenditure by increasing iBAT thermogenesis via SNS. Whether the brain is a target for GCG has been a matter of debate, but others have shown that GCGR signaling in the CNS contributes to the control of energy balance (26,27). Furthermore, the GCGR is expressed in the rat brain (28), and immunohistochemical studies have reported GCG immunoreactivity in the CNS of humans and rodents (29,30). Despite this evidence, the exact neuroanatomical substrate for the control of iBAT metabolism by CNS-GCG signaling remains to be fully characterized.

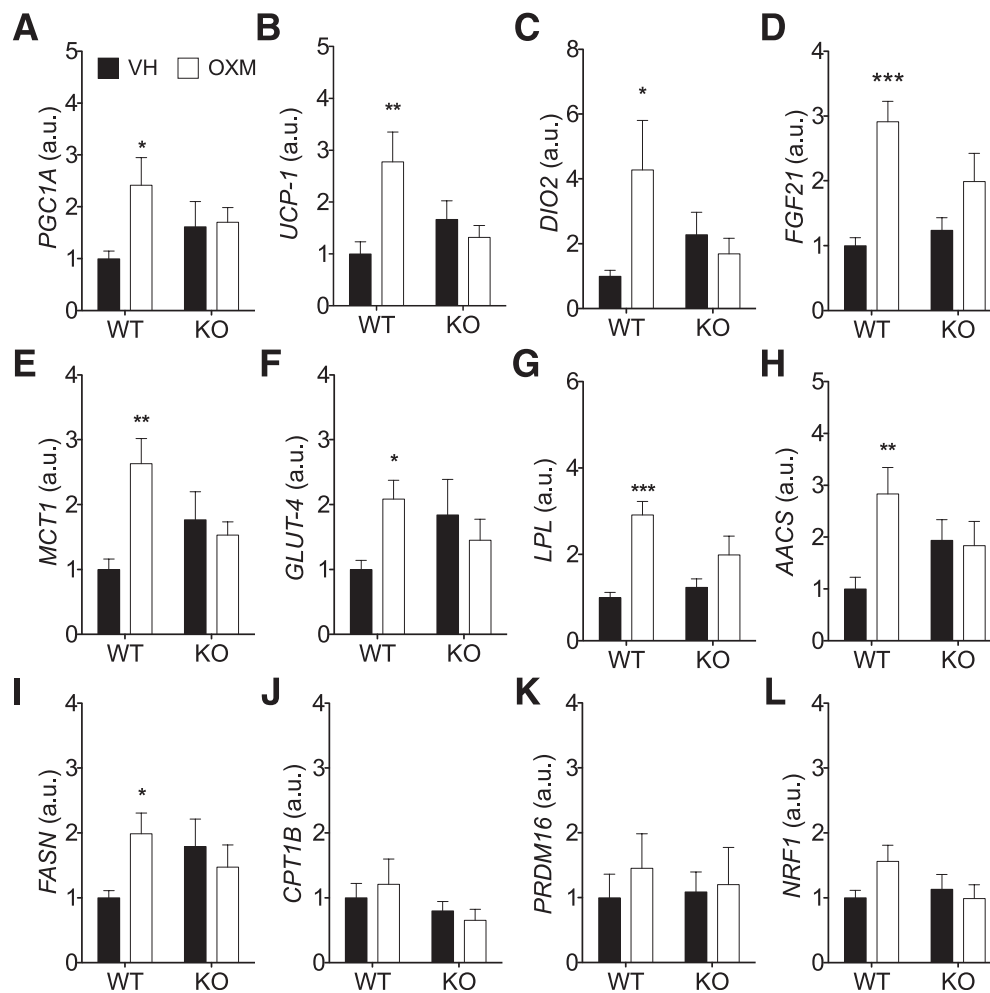OXM may play a role in the control of energy expenditure (12). As yet, no distinct OXM receptor has been

FIG. 5. CNS infusion of OXM increases the expression of genes involved in thermogenesis in the iBAT of WT mice but not in *Glp1r*$^{-/-}$ mice. *PGC1a* (*A*), *UCP-1* (*B*), *DIO2* (*C*), and *FGF21* (*D*) gene expression in BAT is increased in WT but not in GLP-1R knockout mice after 3-day ICV OXM infusion. Similarly, ICV OXM increased the expression of genes involved in energy metabolism, such as *MCT1* (*E*), *GLUT-4* (*F*), *LPL* (*G*), *AACS* (*H*), *FASN* (*I*), *CPT1B* (*J*), *PRDM16* (*K*), and *NRF1* (*L*) in iBAT of WT mice. WT vehicle (VH)-treated mice were pair-fed with the WT OXM group. Data are expressed as means ± SE (*n* = 6–8). **P* < 0.05, ***P* < 0.01, ***P* < 0.001 vs. corresponding vehicle; two-way ANOVA with Bonferroni post hoc test. KO, knockout; a.u., arbitrary unit.

described; its effects have been attributed to its interaction with either GLP-1R or GCGR (7). The increase in the iBAT thermogenesis induced by ICV OXM is consistent with its partial agonism on the GCGR; however, here we show that ICV GLP-1 increases iBAT thermogenesis, and we demonstrate that the classical *Glp1r* is required for the activation of the iBAT by ICV OXM. Surprisingly, we did not see any residual thermogenic effect of ICV OXM in the *Glp1r*$^{-/-}$ mice that could be attributed to activation of the GCGR by OXM. These findings strengthen the role of

the GLP-1R in the control of iBAT thermogenesis; however, we cannot exclude that the GCGR contributes to the iBAT activation induced by ICV OXM in WT mice. Similarly to OXM, GCG can activate the GLP-1R (31), but this requires concentrations well in excess of those used here where we infused GCG, OXM, and GLP-1 in the same molar range. Future studies involving the ICV infusion of OXM and GCG in GCGR-deficient mice may contribute to understanding the specific role of GCGR in the iBAT activation by GCG and OXM.

TABLE 1
Parameters of hyperinsulinemic-euglycemic clamp

	ΔBW (g)	GIR (mg/min/kg)	R_d/HGP (mg/min/kg)	Clamp R_d (mg/min/kg)	Glucose (mmol/L)		Insulin (ng/mL)	
					Basal	Final	Basal	Final
Vehicle	1.2 ± 0.4	49.2 ± 1.7	16.1 ± 1.5	39.8 ± 3.5	6.5 ± 0.4	5.5 ± 0.3	1.5 ± 0.1	9.9 ± 1.1
GLP-1	−2.9 ± 0.2**	66.5 ± 4.3	14.4 ± 0.7	46.5 ± 5.3	5.2 ± 0.3*#	5.8 ± 0.3	1.0 ± 0.1	15.6 ± 1.7^
OXM	−4.1 ± 1.3**	59.7 ± 4.7	16.6 ± 1.3#	47.3 ± 4.4	4.6 ± 0.3**#	6.0 ± 0.4	0.8 ± 0.2	9.2 ± 1.5
Pair fed	−2.5 ± 0.5*	64.6 ± 6.9	11.2 ± 1.2	39.1 ± 5.0	3.8 ± 0.1**	5.2 ± 0.2	0.7 ± 0.3	9.5 ± 1.7

Data are means ± SE. BW, body weight; GIR, glucose infusion rate; HGP, hepatic glucose production. **P* < 0.05 compared with vehicle, ***P* < 0.01 compared with vehicle, #*P* < 0.05 compared with pair fed, ^*P* < 0.05 compared with OXM, one-way ANOVA with Tukey posttest.
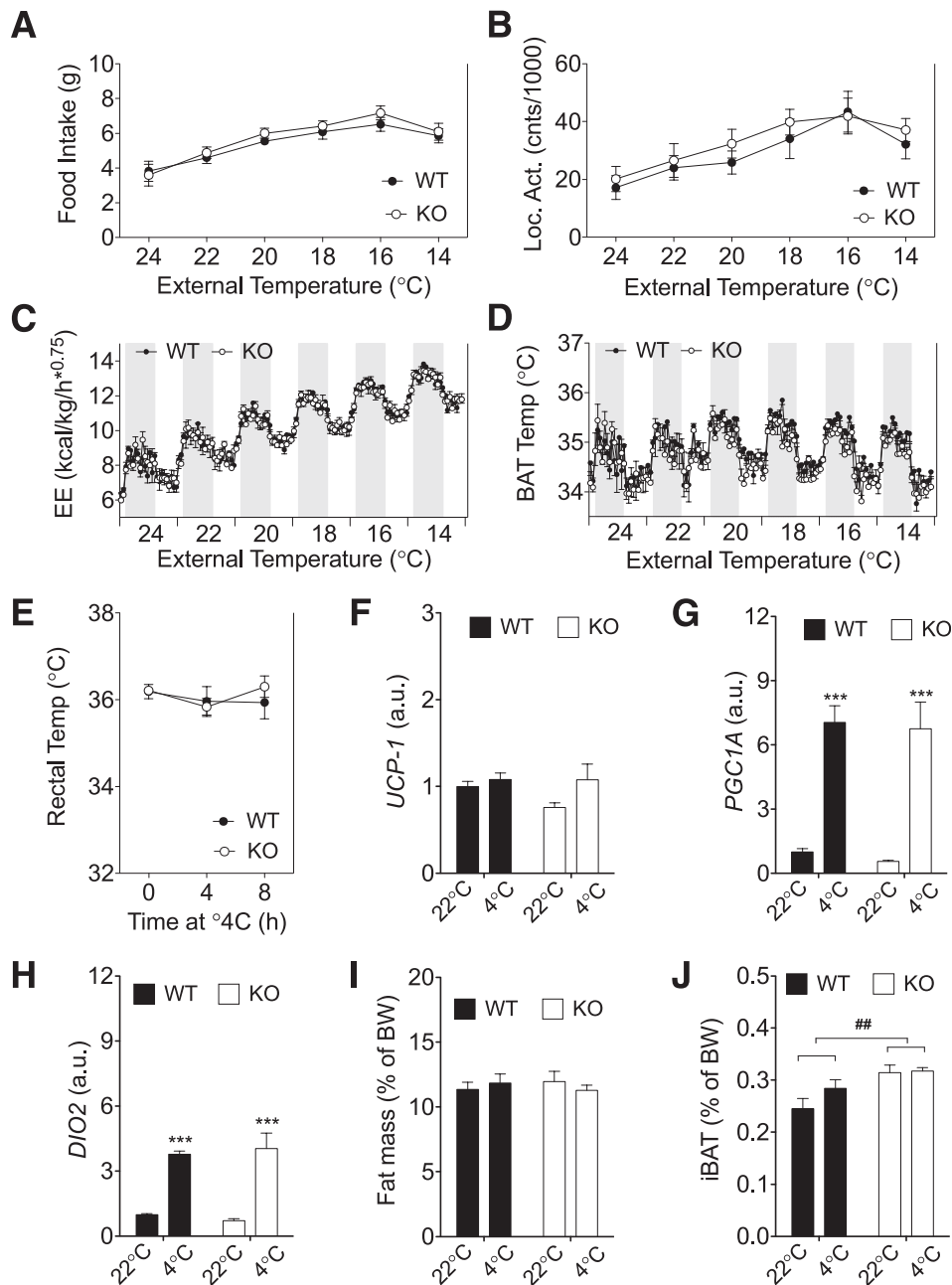
FIG. 6. GLP-1R signaling is not critical for the control of BAT thermogenesis in response to changes in ambient temperature. WT and $Glp1r^{-/-}$ mice implanted with a telemeter temperature transmitter in the iBAT were exposed to decreasing ambient temperature from 24 to 14°C in decrements of 2°C per day. The decrease in ambient temperature led to a similar increase in food intake (A) in both WT and $Glp1r^{-/-}$ mice paralleled by an increase in locomotor activity (Loc. Act) (B) and energy expenditure (EE) (C). Both WT and knockout mice maintained similar iBAT temperature, including circadian-dependent oscillations (D). $E–J$: Response to an acute cold exposure: WT and $Glp1r^{-/-}$ mice fed with standard chow ad libitum and housed always at room temperature were singly housed and exposed to 4°C for 8 h. BCT was measured using a rectal probe (E). Another set of mice was exposed to 4°C for 2 h before euthanasia, while the corresponding control groups were maintained at room temperature. $UCP-1$ (F), $PGC1a$ (G), and $DIO2$ (H) gene expression was assessed in BAT. Fat mass was measured using nuclear magnetic resonance to calculate adiposity (I). iBAT was carefully dissected and weighted (J). Food was removed at the beginning of the cold exposure, which started 2 h after the onset of the light phase. Data are expressed as means ± SE ($A–E$, $n = 8$; $F–J$, $n = 5–6$). ##$P < 0.01$ $Glp1r^{-/-}$ vs. WT; ***$P < 0.001$ vs. corresponding vehicle; two-way ANOVA with Bonferroni post hoc test. Temp, temperature; cnts, counts; KO, knockout.

Interestingly, both OXM and GLP-1 increase iBAT temperature despite inducing a profound anorexia. This is important because food restriction is accompanied by a decrease in iBAT metabolism (Fig. 2J) associated with lower sympathetic signaling (14), which appears to be circumvented after central GLP-1R activation.

There is evidence that CNS–GLP-1 contributes to the control of BCT, although the mechanisms through which it does so are not well characterized. The GLP-1R agonist exendin-4 reduces BCT in conscious rats (32–34) and mice (35). This is, at least in part, attributed to hindbrain GLP-1R signaling (33). Intriguingly, acute intravenous or ICV administration of GLP-1 increases BCT in anesthetized rats (36) and ICV OXM increases rectal temperature in the same animal model (12). OXM does not affect BCT in WT mice but reduces it in dopamine β-hydroxylase–deficient

mice that lack adrenergic signaling (37), raising the possibility that CNS–GLP-1R simultaneously regulates several mechanisms involved in the control of BCT, one of which induces hyperthermia and requires adrenergic signaling. Our data suggest that this is iBAT thermogenesis.

The GLP-1R–dependent increase in iBAT thermogenesis induced by ICV OXM is consistent with both the increase in iBAT SNS activity and the expression changes in iBAT genes that reflect increased adrenergic signal, namely, increased levels of PGC1a, UCP-1, DIO2, and FGF21 (Fig. 5A–C). Hepatic FGF21 contributes to the activation of iBAT thermogenesis in neonates (38) and in iBAT increases after cold exposure in vivo or after incubation of brown adipocytes with adrenergic receptor agonists in vitro (39,40); however, the role of BAT-derived FGF21 remains to be fully elucidated. ICV OXM also increased the expression of genes involved in the uptake of metabolic substrates from the extracellular space, such as MCT-1, GLUT4, and LPL. MCT-1 is the most abundant monocarboxylate transporter in iBAT (41) and regulates the uptake of lactate and ketone bodies. The increase in GLUT4 expression suggests that CNS–GLP-1 signaling contributes to increased insulin-stimulated glucose uptake in BAT. This is supported by recent data showing that a long-lasting GLP-1 agonist similarly increases insulin responsiveness in this tissue (42). Cold exposure increases plasma triglyceride uptake (43), as well as lipogenesis in iBAT (44,45). Thus, the increased expression of LPL, AACS, and FASN after ICV OXM in WT mice further supports the role of SNS mediating the CNS–GLP-1R control of iBAT metabolism. Interestingly, $Glp1r^{-/-}$ mice have increased percentage of iBAT mass per mouse. Although the cause of this increase remains to be elucidated, it is consistent with a decreased SNS tone in iBAT, given that mice with impaired adrenergic signaling have larger iBAT (46,47). In view of the CNS–GLP-1R induction of iBAT thermogenesis, we tested the importance of this receptor in overall thermoregulatory control by challenging WT mice and GLP-1R–deficient littermates with cold exposure. $Glp1r^{-/-}$ mice maintained appropriate iBAT thermogenesis and BCT in response to cold exposure. Thus, assuming that $Glp1r^{-/-}$ mice do not display any compensatory adaptation for the congenital loss of GLP-1R, we can conclude that GLP-1R signaling is not essential to regulate homeothermia.

In summary, in this study, we demonstrate that both GCGR and GLP-1R action in the CNS control iBAT thermogenesis. Although GLP-1R is not essential for homeothermic control in response to ambient cold, it uses the common efferent mechanisms, namely, the SNS, to increase iBAT thermogenesis. We propose that iBAT thermogenesis is one of the multiple mechanisms by which, along with the control of feeding and WAT metabolism, pharmacological CNS–GLP-1R contributes to the maintenance of energy balance.

REFERENCES

1. Wren AM, Bloom SR. Gut hormones and appetite control. Gastroenterology 2007;132:2116–2130
2. Astrup A, Rössner S, Van Gaal L, et al.; NN8022-1807 Study Group. Effects of liraglutide in the treatment of obesity: a randomised, double-blind, placebo-controlled study. Lancet 2009;374:1606–1616
3. Kanoski SE, Fortin SM, Arnold M, Grill HJ, Hayes MR. Peripheral and central GLP-1 receptor populations mediate the anorectic effects of peripherally administered GLP-1 receptor agonists, liraglutide and exendin-4. Endocrinology 2011;152:3103–3112
4. Heppner KM, Habegger KM, Day J, et al. Glucagon regulation of energy metabolism. Physiol Behav 2010;100:545–548
5. Pocai A, Carrington PE, Adams JR, et al. Glucagon-like peptide 1/glucagon receptor dual agonism reverses obesity in mice. Diabetes 2009;58:2258–2266
6. Day JW, Ottaway N, Patterson JT, et al. A new glucagon and GLP-1 co-agonist eliminates obesity in rodents. Nat Chem Biol 2009;5:749–757
7. Baggio LL, Huang QL, Brown TJ, Drucker DJ. Oxyntomodulin and glucagon-like peptide-1 differentially regulate murine food intake and energy expenditure. Gastroenterology 2004;127:546–558
8. Parlevliet ET, Heijboer AC, Schröder-van der Elst JP, et al. Oxyntomodulin ameliorates glucose intolerance in mice fed a high-fat diet. Am J Physiol Endocrinol Metab 2008;294:E142–E147
9. Dakin CL, Gunn I, Small CJ, et al. Oxyntomodulin inhibits food intake in the rat. Endocrinology 2001;142:4244–4250
10. Wynne K, Park AJ, Small CJ, et al. Subcutaneous oxyntomodulin reduces body weight in overweight and obese subjects: a double-blind, randomized, controlled trial. Diabetes 2005;54:2390–2395
11. Maida A, Lovshin JA, Baggio LL, Drucker DJ. The glucagon-like peptide-1 receptor agonist oxyntomodulin enhances beta-cell function but does not inhibit gastric emptying in mice. Endocrinology 2008;149:5670–5678
12. Dakin CL, Small CJ, Park AJ, Seth A, Ghatei MA, Bloom SR. Repeated ICV administration of oxyntomodulin causes a greater reduction in body weight gain than in pair-fed rats. Am J Physiol Endocrinol Metab 2002;283:E1173–E1177

13. Billington CJ, Bartness TJ, Briggs J, Levine AS, Morley JE. Glucagon stimulation of brown adipose tissue growth and thermogenesis. Am J Physiol 1987;252:R160–R165

14. Cannon B, Nedergaard J. Brown adipose tissue: function and physiological significance. Physiol Rev 2004;84:277–359

15. Nogueiras R, Pérez-Tilve D, Veyrat-Durebex C, et al. Direct control of peripheral lipid deposition by CNS GLP-1 receptor signaling is mediated by the sympathetic nervous system and blunted in diet-induced obesity. J Neurosci 2009;29:5916–5925

16. Cypess AM, Lehman S, Williams G, et al. Identification and importance of brown adipose tissue in adult humans. N Engl J Med 2009;360:1509–1517

17. van Marken Lichtenbelt WD, Vanhommerig JW, Smulders NM, et al. Cold-activated brown adipose tissue in healthy men. N Engl J Med 2009;360:1500–1508

18. Virtanen KA, Lidell ME, Orava J, et al. Functional brown adipose tissue in healthy adults. N Engl J Med 2009;360:1518–1525

19. Scrocchi LA, Brown TJ, MaClusky N, et al. Glucose intolerance but normal satiety in mice with a null mutation in the glucagon-like peptide 1 receptor gene. Nat Med 1996;2:1254–1258

20. Lockie SH, Czyzyk TA, Chaudhary N, et al. CNS opioid signaling separates cannabinoid receptor 1-mediated effects on body weight and mood-related behavior in mice. Endocrinology 2011;152:3661–3667

21. Turton MD, O'Shea D, Gunn I, et al. A role for glucagon-like peptide-1 in the central regulation of feeding. Nature 1996;379:69–72

22. Burcelin R, Crivelli V, Dacosta A, Roy-Tirelli A, Thorens B. Heterogeneous metabolic adaptation of C57BL/6J mice to high-fat diet. Am J Physiol Endocrinol Metab 2002;282:E834–E842

23. Heim T, Hull D. The effect of propranolol on the calorigenic response in brown adipose tissue of new-born rabbits to catecholamines, glucagon, corticotrophin and cold exposure. J Physiol 1966;187:271–283

24. Kuroshima A, Yahata T. Thermogenic responses of brown adipocytes to noradrenaline and glucagon in heat-acclimated and cold-acclimated rats. Jpn J Physiol 1979;29:683–690

25. Dicker A, Zhao J, Cannon B, Nedergaard J. Apparent thermogenic effect of injected glucagon is not due to a direct effect on brown fat cells. Am J Physiol 1998;275:R1674–R1682

26. Inokuchi A, Oomura Y, Nishimura H. Effect of intracerebroventricularly infused glucagon on feeding behavior. Physiol Behav 1984;33:397–400

27. Kurose Y, Kamisoyama H, Honda K, et al. Effects of central administration of glucagon on feed intake and endocrine responses in sheep. Anim Sci J 2009;80:686–690

28. Hoosein NM, Gurd RS. Identification of glucagon receptors in rat brain. Proc Natl Acad Sci USA 1984;81:4368–4372

29. Dorn A, Rinne A, Bernstein HG, Hahn HJ, Ziegler M, Dammert K. Immunoreactive glucagon in neurons of various parts of the human brain. Demonstration by immunofluorescence technique. Acta Histochem 1981;69:243–247

30. Jin SLC, Han VKM, Simmons JG, Towle AC, Lauder JM, Lund PK. Distribution of glucagonlike peptide I (GLP-I), glucagon, and glicentin in the rat brain: an immunocytochemical study. J Comp Neurol 1988;271:519–532

31. Runge S, Wulff BS, Madsen K, Bräuner-Osborne H, Knudsen LB. Different domains of the glucagon and glucagon-like peptide-1 receptors provide the critical determinants of ligand selectivity. Br J Pharmacol 2003;138:787–794

32. Skibicka KP, Alhadeff AL, Grill HJ. Hindbrain cocaine- and amphetamine-regulated transcript induces hypothermia mediated by GLP-1 receptors. J Neurosci 2009;29:6973–6981

33. Hayes MR, Skibicka KP, Grill HJ. Caudal brainstem processing is sufficient for behavioral, sympathetic, and parasympathetic responses driven by peripheral and hindbrain glucagon-like-peptide-1 receptor stimulation. Endocrinology 2008;149:4059–4068

34. O'Shea D, Gunn I, Chen X, Bloom S, Herbert J. A role for central glucagon-like peptide-1 in temperature regulation. Neuroreport 1996;7:830–832

35. Griffioen KJ, Wan R, Okun E, et al. GLP-1 receptor stimulation depresses heart rate variability and inhibits neurotransmission to cardiac vagal neurons. Cardiovasc Res 2011;89:72–78

36. Osaka T, Endo M, Yamakawa M, Inoue S. Energy expenditure by intravenous administration of glucagon-like peptide-1 mediated by the lower brainstem and sympathoadrenal system. Peptides 2005;26:1623–1631

37. Sowden GL, Drucker DJ, Weinshenker D, Swoap SJ. Oxyntomodulin increases intrinsic heart rate in mice independent of the glucagon-like peptide-1 receptor. Am J Physiol Regul Integr Comp Physiol 2007;292:R962–R970

38. Hondares E, Rosell M, Gonzalez FJ, Giralt M, Iglesias R, Villarroya F. Hepatic FGF21 expression is induced at birth via PPARalpha in response to milk intake and contributes to thermogenic activation of neonatal brown fat. Cell Metab 2010;11:206–212

39. Chartoumpekis DV, Habeos IG, Ziros PG, Psyrogiannis AI, Kyriazopoulou VE, Papavassiliou AG. Brown adipose tissue responds to cold and adrenergic stimulation by induction of FGF21. Mol Med 2011;17:736–740

40. Hondares E, Iglesias R, Giralt A, et al. Thermogenic activation induces FGF21 expression and release in brown adipose tissue. J Biol Chem 2011;286:12983–12990

41. Iwanaga T, Kuchiiwa T, Saito M. Histochemical demonstration of monocarboxylate transporters in mouse brown adipose tissue. Biomed Res 2009;30:217–225

42. Gu W, Lloyd DJ, Chinookswong N, et al. Pharmacological targeting of glucagon and glucagon-like peptide 1 receptors has different effects on energy state and glucose homeostasis in diet-induced obese mice. J Pharmacol Exp Ther 2011;338:70–81

43. Bartelt A, Bruns OT, Reimer R, et al. Brown adipose tissue activity controls triglyceride clearance. Nat Med 2011;17:200–205

44. Jakus PB, Sandor A, Janaky T, Farkas V. Cooperation between BAT and WAT of rats in thermogenesis in response to cold, and the mechanism of glycogen accumulation in BAT during reacclimation. J Lipid Res 2008;49:332–339

45. Yu XX, Lewin DA, Forrest W, Adams SH. Cold elicits the simultaneous induction of fatty acid synthesis and beta-oxidation in murine brown adipose tissue: prediction from differential gene expression and confirmation in vivo. FASEB J 2002;16:155–168

46. Thomas SA, Palmiter RD. Thermoregulatory and metabolic phenotypes of mice lacking noradrenaline and adrenaline. Nature 1997;387:94–97

47. Bachman ES, Dhillon H, Zhang CY, et al. betaAR signaling required for diet-induced thermogenesis and obesity resistance. Science 2002;297:843–845